Table II. Quantum Yields for Dimerization of **1a** in Various Conditions

solvent	concn (mol/L)	$\Phi_{dim.}$ ($\times 10^{-2}$)
C_6H_6	0.005	0.3
C_6H_6	0.01	0.6
C_6H_6	0.02	1.3
C_6H_6	0.03	1.4
C_6H_6	0.04	1.5
C_6H_6	0.10	1.5
Et_2O	0.02	1.0
CH_3CN	0.02	0.7

Irradiation of a benzene solution of **1a** (0.02 M) with a high-pressure mercury lamp through a Pyrex filter under argon gave two photoproducts. They were isolated by flash column chromatography and identified as the dimer, 3,12-dicyano-4,8-dimethoxy-1,6-dimethyl-5,9-diazatetracyclo[4.3.3.$0^{2,7}$.$0^{3,10}$]dodeca-4,8-diene (**2a**), and the transpositional isomer **3a**. Photolysis of other pyridines (**1b** and **1c**) gave the results shown in Table I. The structure of **2b** was confirmed by X-ray structural analysis (Figure 1).

When **1a** and **1b** were irradiated at a concentration above 0.04 M, the corresponding dimers (**2a** and **2b**) were obtained as sole photoproducts. In contrast to the photoreactions of the monomethylated pyridines (**1a-1c**), those of 3-cyano-4,6-dimethyl-2-methoxy- and -2-ethoxypyridine (**1d** and **1e**) did not give the dimers but formed the transpositional isomers (**3d** and **3e**) almost quantitatively. When **1d** and **1e** were irradiated at a higher concentration (0.1 M), the corresponding dimers were not detected. The difference in reactivity might be attributed to the steric effect of a methyl group at 4-position.

For the formation of the dimer (**2**), a mechanism is postulated that involves [$2\pi + 2\pi$] photodimerization between C5-C6 and C2'-C3' bonds followed by [$2\pi + 2\pi + 2\pi + 2\sigma$] rearrangement (Scheme I). The rearrangement probably results from the weakened character of the carbon-carbon bond of the cyclobutane ring caused by donor-acceptor conjugation. The trapping of cyclobutane-type intermediate **4** with dienophiles was unsuccessful. The formation of the transpositional isomer **3** is reasonably explainable in terms of a 1,3-shift via Dewar pyridine.[6]

The photocycloadditions of many aromatic compounds proceed via exciplex or excimer. At a concentration of about 10^{-4} M or less, the fluorscence of **1a** was concentration-independent and was composed of pure pyridine monomer fluorescence. As the pyridine concentration increased, the monomer emission decreased in intensity; however, a new fluorescence emission due to the pyridine excimer was not observed. There was no change caused by pyridine concentration in the absorption spectra. The dimerizations were not sensitized by 3-methoxyacetophenone (E_T 72.4 kcal/mol).[7] Quenching of the dimerizations by 2,5-dimethylhexa-2,4-diene (E_T 58.7 kcal/mol)[7] or *trans*-stilbene (E_T 50 kcal/mol)[7] was quite inefficient. These results indicate that the photodimerizations proceed from the singlet excited states. The quantum yields were dependent upon the pyridine concentration, and the maximum was 1.5×10^{-2} at concentrations above 0.04 M[8] (Table II). Furthermore, it seems that a nonpolar solvent is preferred for the dimerization.

Whereas 2-pyridones[9] and 2-aminopyridinium ions[10] form well-known [$4\pi + 4\pi$] dimers on irradiation, pyridines, quinolines, and isoquinolines are generally unreactive toward addition reactions.[11] Although both inter- and intramolecular [$4\pi + 4\pi$] cycloadditions of naphthalenes[12] and anthracenes[13] have been studied extensively, there is no example of [$2\pi + 2\pi$] dimerization of six-membered monocyclic aromatic compounds, to our knowledge. The photoreaction of 3-cyano-2-methoxy-6-methylpyridines provides an unprecedented cyclodimerization in pyridine photochemistry. We are continuing to explore the scope and limitations of the photodimerization of heteroaromatics.

(6) (a) Caplain, S.; Lablache-Combier, A. *J. Chem. Soc., Chem. Commun.* **1970**, 1247. (b) Chambers, R. D.; Middleton, R. *J. Chem. Soc., Perkin Trans. 1* **1977**, 1500.

(7) Murov, S. L. *Handbook of Photochemistry*; Marcel Dekker: New York, 1973.

(8) A valerophenone actinometer was used: Wagner, P. J.; Kelso, P. A.; Zepp, R. G. *J. Am. Chem. Soc.* **1972**, *94*, 7480.

(9) (a) Paquette, L. A.; Slomp, G. *J. Am. Chem. Soc.* **1963**, *85*, 765. (b) Taylor, E. C.; Kan, R. O. *J. Am. Chem. Soc.* **1963**, *85*, 776.

(10) (a) Bendig, J.; Buchwitz, W.; Fischer, J.; Kreysig, D. *J. Prakt. Chem.* **1981**, 323, 485. (b) Julian, D. R. *Photochemistry of Heterocyclic Compounds*; Horspool, W. M., Ed.; Wiley: New York, 1976; Chapter 9 and references therein.

(11) Photochemical hydrogen abstraction and substitution reactions of heteroaromatic nitrogen compounds have been reported. (a) Beak, P.; Messer, W. R. *Organic Photochemistry*; Chapman, O. L., Ed.; Marcel Dekker: New York, 1967: Vol. 1, 117. (b) Cornelisse, J.; Havinga, E. *Chem. Rev.* **1975**, *75*, 353. (c) Combier, A. L. *Photochemistry of Heterocyclic Compounds*; Buchardt, O., Ed.; John Wiley & Sons: New York, London, Sydney, and Toronto; 1976; Chapter 4. (d) Whitten, D. G. *Ibid.* Chapter 8. (e) Mariano, P. S. *Organic Photochemistry*; Padwa, A., Ed.; Marcel Dekker: New York and Basal, 1987; Vol. 9. (f) Marlkin, Y. N.; Kuz'min, V. A. *Russ. Chem. Rev.* **1990**, *59*, 164. See also ref 1a.

(12) (a) Seliger, B. K.; Sterns, M. *J. Chem. Soc., Chem. Commun.* **1969**, 978. (b) Mattingly, T. W.; Lancaster, J. E.; Zweig, A. *J. Chem. Soc., Chem. Commun.* **1971**, 595. (c) Kowala, C.; Sugowdz, G.; Sasse, W. H. F.; Wunderlich, J. A. *Tetrahedron Lett.* **1972**, 4721. (d) Teitei, T.; Wells, D.; Spurling, T.; Sasse, W. H. F. *Aust. J. Chem.* **1978**, *31*, 85. (e) Albini, A.; Giannantonia, L. *J. Org. Chem.* **1984**, *49*, 3863.

(13) (a) Fritsche, J. *J. Prakt. Chem.* **1867**, *101*, 333. (b) Bouas-Laurent, H.; Castellan, A.; Desvergue, J.-P. *Pure Appl. Chem.* **1980**, *52*, 2633.

An Algorithm for the Systematic Solvation of Proteins Based on the Directionality of Hydrogen Bonds

Angelo Vedani*

Biographics Laboratory, Swiss Institute for Alternatives to Animal Testing (SIAT) Aeschstrasse 14, CH-4107 Ettingen, Switzerland

David W. Huhta

Department of Biochemistry, The University of Kansas Lawrence, Kansas 66045

Received February 21, 1991

We present the development of an algorithm for the systematic solvation of proteins based on the directionality of H bonds.[1-4] By analysis of the distribution and environment of H-bond donors and acceptors of a protein, positions for both internal and surface water molecules are identified. The algorithm was incorporated into the program AUTO-SOL, which is part of the molecular mechanics software "Yeti". In detail, the algorithm includes the following steps:

1. Linearity of H bonds is represented by H-extension vectors (HEVs), H-bond directionality by lone-pair vectors (LPVs). HEVs originate at H-bond donors, LPVs at H-bond acceptors. The end point of a HEV marks the ideal position for a H-bond acceptor atom relative to the H-bond donor fragment. The end point of a LPV marks the ideal position for a H-bond donor atom relative to the H-bond acceptor fragment. Length and orientation of HEVs and LPVs were derived from analyses of H-bond geometries in small-molecule crystal structures.[1-4]

To identify free HEVs and LPVs, able to engage in H bonds with additional water molecules, it is necessary to delete those vectors associated with already existing hydrogen bonds. Ideally, the HEV and LPV of a particular H bond would overlap entirely, but this is rarely observed in protein structures.[5] LPVs and HEVs

(1) Murray-Rust, P.; Glusker, J. P. *J. Am. Chem. Soc.* **1984**, *106*, 1018-1025.

(2) Taylor, R.; Kennard, O. *Acc. Chem. Res.* **1984**, *17*, 320-326.

(3) Vedani, A.; Dunitz, J. D. *J. Am. Chem. Soc.* **1985**, *107*, 7653-7658.

(4) Alexander, R. S.; Kanyo, Z. F.; Chirlian, L. E.; Christianson, D. W. *J. Am. Chem. Soc.* **1990**, *112*, 933-937.

0002-7863/91/1513-5860$02.50/0

Table I. Reproduction of Protein-Bound Water Molecules Using the "Yeti" Module AUTO-SOL

	protein[a]				
	3PTN	4EST	3TLN	3GRS	1CSE
resolution, Å	1.7	1.65	1.6	1.54	1.2
water molecules, X-ray	82	127	173	523	432
metal-bound solvent[b]	2	1	9	0	2
non-metal-bound solvent	80	126	164	523	430
engaged in H bonds[c] (protein and solvent)	77	110	152	420	321
engaged in H bonds with the protein[c]	67	101	122	245	170
engaged in more than one H bond with the protein[c]	27	38	38	60	33
Crystallographic Water Molecules[d]					
$d < 0.5$ Å	16	23	25	40	30
0.5 Å $< d <$ 1.0 Å	31	40	47	134	92
1.0 Å $< d <$ 1.5 Å	19	37	46	177	98
1.5 Å $< d <$ 2.0 Å	10	16	28	85	83
2.0 Å $< d <$ 2.5 Å	2	5	12	46	44
2.5 Å $< d <$ 3.0 Å	2	4	3	30	26
$d > 3.0$ Å	0	1	3	11	57
% within 1.5 Å	83	79	72	67	51
Tightly Bound Crystallographic Water Molecules[e]					
$d < 0.5$ Å	7	10	11	10	5
0.5 Å $< d <$ 1.0 Å	14	18	13	28	20
1.0 Å $< d <$ 1.5 Å	3	5	12	18	7
$d < 1.5$ Å	3	5	2	4	1
% within 1.5 Å	89	87	95	93	97

[a] Brookhaven Protein Data Bank[8] code: 3PTN, native trypsin (bovine);[9] 4EST, native elastase (porcine);[10] 3TLN, native thermolysin (*Bacillus thermoproteolyticus*);[11] 3GRS, native glutathione reductase (human);[12] 1CSE, subtilisin complex with eglin C (Carlsberg).[13] [b] Reproduction of metal-bound water molecules was not attempted since their number and orientation depend on coordination number and coordination type at the metal center. [c] Using the "Yeti" force field[6] as the determining criterion. [d] Number of crystallographic water molecules for which a water molecule, generated by AUTO-SOL, is found within the given distance range. [e] Number of tightly bound crystallographic water molecules (engaging in two or more H bonds with the protein) for which a water molecule, generated by AUTO-SOL, is found within the given distance range.

are therefore extended to a cone, representing the experimental distribution width (cf. refs 1–4). Criteria for identifying "existing" H bonds are then based on the Yeti force field.[6]

2. In the next step, the remaining vectors are analyzed for clustering. Probable sites for water molecules (i.e., the position of their O atom) are searched in regions of 3-D space where at least two vectors' end points (HEVs or LPVs) are located within a short distance. The maximum vector separation was limited to 1.4 Å, corresponding to half the length of a water–water H bond. An initial position for the water O atom is then assigned to the midpoint between the two vector tips. Ideally, the angle subtended by the two vectors would lie in the range from 104.5° (H–O–H angle; the water molecule donates two H bonds to the protein) to 114.4° (LP–O–LP angle; the water molecule accepts two H bonds from the protein). AUTO-SOL allows a maximal deviation of 45° from ideality. As a third criterion, the program evaluates the deviation of the two newly formed water–protein H bonds from ideal directionality; a maximum deviation of 30° is accepted.

Next, the environment of this putative water O atom position is scanned for close contacts using van der Waals and H-bond parameters as defined in the "Yeti" force field.[6] If unreasonably short contacts are encountered, the water site is rejected.

3. Finally, the water molecule is oriented along the HEVs (water lone pairs) and/or LPVs (water H atoms) that were used to generate its O atom position.

Because each H-bond donor and acceptor of the protein is systematically analyzed, AUTO-SOL is able to identify internal protein-bound solvent. As we showed in an earlier study,[7] internal solvent is of utmost importance for molecular-mechanical simulations. The structure of a solvent shell generated by AUTO-SOL is most sensitive to the parameters defining the acceptable cavity, i.e., the van der Waals and H-bond parameters of the "Yeti" force field.[6] A general limitation of the program in its present form is the solvation of larger hydrophobic regions exposed to the solvent, since only few HEVs or LPVs originate at such residues.

To test the algorithm, we performed a simulation aimed at reproducing the crystallographically identified solvent of five high-resolution protein crystal structures: trypsin, elastase, thermolysin, glutathione reductase, and subtilisin, all of which were retrieved from the Brookhaven Protein Data Bank.[8] For these five proteins, AUTO-SOL reproduces an average of 70% of the crystallographic solvent within 1.5 Å—half the length of a H bond—of the experimental position. When analyzing tightly bound crystallographic solvent (defined as those water molecules engaging in two or more H bonds with the protein), AUTO-SOL is able to reproduce an average of 92% within 1.5 Å of the experimental position (cf. Table I).

The best results were obtained for trypsin and elastase (for 83% and 79% of their crystallographic solvent, respectively, a water molecule generated by AUTO-SOL is located within 1.5 Å of the experimental position); thermolysin and glutathione reductase yielded satisfactory results (72% and 67%, respectively). The relatively modest value obtained for subtilisin (51%) may be explained by the fact that only 39% of the crystallographic solvent of subtilisin engages in H bonds with the protein (cf. Table I) when the "Yeti" force field[6] is used as a criterion. Tightly bound water molecules are reproduced about equally well for all five proteins (87–97%).

Nonprofit organizations may obtain a copy of the program AUTO-SOL (as part of the molecular mechanics software "Yeti" at prime cost. Details for the distribution should be requested from the author of the program (A.V.).

(5) Baker, E. N.; Hubbard, R. E. *Prog. Biophys. Mol. Biol.* **1984**, *44*, 97–179.
(6) Vedani, A.; Huhta, D. W. *J. Am. Chem. Soc.* **1990**, *112*, 4759–4767.
(7) Vedani, A.; Huhta, D. W.; Jacober, S. P. *J. Am. Chem. Soc.* **1989**, *111*, 4075–4081.
(8) Bernstein, F.; Koetzle, T. F.; Williams, G. J. B.; Meyer, E. F., Jr.; Brice, M. D.; Rodgers, J. R.; Kennard, O.; Shimanouchi, T.; Tasumi, M. J. *J. Mol. Biol.* **1977**, *112*, 535.
(9) Walter, J.; Steigemann, W.; Singh, T. P.; Bartunik, H.; Bode, W.; Huber, R. *Acta Crystallogr., Sect. B* **1982**, *38*, 1462–1472.
(10) Meyer, E. F., Jr.; Cole, G.; Radahakrishnan, R.; Epp, O. *Acta Crystallogr., Sect. B* **1988**, *44*, 26–37.
(11) Holmes, M. A.; Matthews, B. W. *J. Mol. Biol.* **1982**, *160*, 623–639.
(12) Karplus, P. A.; Schulz, G. E. *J. Mol. Biol.* **1987**, *195*, 701–729.
(13) Bode, W.; Papamokos, E.; Musil, D. *Eur. J. Biochem.* **1987**, *166*, 673–692.

Acknowledgment. We express our gratitude to Stephen P. Jacober for stimulating discussions and validating parts of the concept. We gratefully acknowledge financial support from the "Foundation for the Replacement of Animals in Medical Research" (FFVFF), Switzerland, and the "Swiss Institute for Alternatives to Animal Testing" (SIAT). D.W.H. is a NIH Predoctoral trainee under PHS Grant GM-07775.

Exchange of Dinitrogen between Iron and Molybdenum Centers and the Reduction of Dinitrogen Bound to Iron: Implications for the Chemistry of Nitrogenases

G. J. Leigh* and M. Jimenez-Tenorio

AFRC IPSR Nitrogen Fixation Laboratory
University of Sussex, Brighton BN1 9RQ, U.K.
Received December 17, 1990

The recent discovery of the vanadium-iron nitrogenase[1] and of a nitrogenase that apparently contains only iron[2] suggests that vanadium and iron, as well as molybdenum of the conventional nitrogenase,[3,4] may mediate the reduction of dinitrogen in vivo. We present here chemical data that show that the metal species common to the three nitrogenases, namely, iron, is itself capable of mediating the reduction of dinitrogen under mild conditions in vitro. This would lend support to the contention that iron may constitute the active site in all kinds of nitrogenases.

We have recently prepared the iron(II) dinitrogen complex $[FeH(N_2)(dmpe)_2]^+$ (dmpe = 1,2-bis(dimethylphosphino)ethane) by direct reaction of N_2 with $[FeH(H_2)(dmpe)_2]^+$.[5] This N_2 complex reacts with bases such as KOBu^t to produce an unstable iron(0) complex which we formulate as $[Fe(N_2)(dmpe)_2]$. This

$$[FeH(N_2)(dmpe)_2]^+ \xrightarrow{OBu^{t-}} [Fe(N_2)(dmpe)_2] + Bu^tOH$$

product has been characterized in solution by IR spectroscopy and $^{31}P\{^1H\}$ spectroscopy. (IR: $\nu(^{14}N_2)$ 1975, $\nu(^{15}N_2)$ 1917 cm^{-1}, THF. $^{31}P\{^1H\}$ NMR (THF/C_6D_6) A_2B_2 system, P_A -60.02, P_B -74.17 ppm (P(OMe) standard), $^2J_{PP}$ = 26 Hz.) This compound slowly loses N_2, and if the deprotonation is carried out under vacuum or zero partial pressure of N_2, all N_2 is rapidly lost. However, treatment of the solution of $[Fe(N_2)(dmpe)_2]$ with acids yields ammonia, and this was estimated quantitatively after base distillation, as shown in Table I. An approximately molar solution of HCl in Et_2O was generated from Me_3SiCl and MeOH, and this was used to ensure an HCl:Fe ratio of ca. 10:1. Because of the lability of the N_2 in $[Fe(N_2)(dmpe)_2]$, we were unable to devise a method to obtain a nitrogen balance in dinitrogen plus ammonia, but with HCl the ultimate iron product is $[FeCl_2(dmpe)_2]$ as determined by IR, UV, and $^{31}P\{^1H\}$ NMR spectroscopy and comparison with an authentic sample. The yield of $[FeCl_2(dmpe)_2]$ is of the order of 80%, but the dichloro complex itself reacts slowly with HCl. This system under optimal conditions can supply only two electrons per dinitrogen since the iron changes from iron(0) to iron(II), so that the maximum yield of ammonia should be $^2/_3NH_3$/initial mole of $[FeH(N_2)(dmpe)_2]^+$. Our best yields are currently of the order of 18%, but yields have yet to be optimized (Table I). Only trace amounts of hydrazine were observed, and then only in the presence of magnesium chloride, which was added in order to parallel some systems in which metal-N_2-magnesium interactions have been observed.[6] Protonation reactions carried out in vacuo yielded N_2 and H_2, 1 molar equiv of each.

Table I

compd or system	solvent[a]/acid	concn[b] of recovered NH_3, mM	yield[c] of NH_3, %
$[FeH(N_2)(dmpe)_2][BPh_4]$	THF/HCl	0	0
$[FeH(N_2)(dmpe)_2][BPh_4]$	THF/H_2SO_4	1.4	3.6
$[FeH(N_2)(dmpe)_2][BPh_4]$ + LiPh (5 molar equiv)	THF/H_2SO_4	1.0	2.6
$[Fe(N_2)(dmpe)_2]$	THF/H_2SO_4	3.4	8.6
$[Fe(N_2)(dmpe)_2]$	THF/HCl	4.8	12
$[Fe(N_2)(dmpe)_2]$	Et_2O/HCl	3.8	9.6
$[Fe(N_2)(dmpe)_2]$[d] + $MgCl_2$ (10 molar equiv)	THF/HCl	2.6	6.6

[a] THF = tetrahydrofuran. [b] Concentration of solution after base distillation and making up to 25 cm^3 starting from 1 mmol of Fe complex. Ammonia determination by the indophenol test. These values are corrected for blanks consisting of $[FeH(H_2)(dmpe)_2][BPh_4]$ treated as necessary with base and/or acid in the appropriate solvent under argon. Under such circumstances background concentrations of ca. 0.15 mM ammonia were obtained. [c] Yield expressed as (moles of NH_3/moles of $[FeH(N_2)(dmpe)_2][BPh_4]$) × 100. In terms of electrons, these yields need to be multiplied by $^3/_2$, since $Fe^0 \rightarrow Fe^{II}$ provides two electrons and $^1/_2N_2 \rightarrow NH_3$ requires three. [d] In only this case was any hydrazine observed (*p*-(dimethylamino)benzaldehyde test). Yield 0.4% based on initial iron complex.

Scheme I

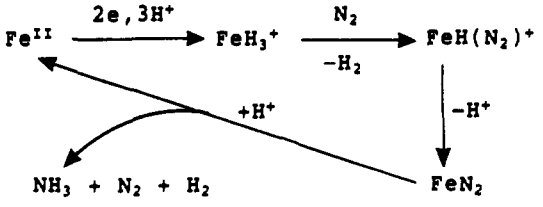

These results show that it is possible to construct a reductive cycle for dinitrogen on iron solely by changing the hydrogen ion concentration (Scheme I).

We do not yet understand the mechanistic details of these reactions, but the system differs significantly from any iron nitrogen-fixing systems in the literature,[7] all of which employ strong reducing agents such as Grignard reagents, as well as nonprotic media. Our system does not require a reducing agent stronger than borohydride, which can function in protic solvents such as alcohols, and the effect of which could be mimicked in a protein by changing the relative fluxes of protons and electrons reaching a metal center.

We attempted to make compounds containing dinitrogen bridging between iron and molybdenum[8] by reaction of $[FeH(H_2)(dmpe)_2]^+$ with $[Mo(N_2)_2(dppe)_2]$ (dppe = 1,2-bis(diphenylphosphino)ethane) under Ar in tetrahydrofuran. What we observed is the metathetical reaction shown below, the known products being recovered in about 70% yield, but as judged by IR spectroscopy, the reaction appears quantitative.

$$2[FeH(H_2)(dmpe)_2]^+ + [Mo(N_2)_2(dppe)_2] \rightarrow 2[FeH(N_2)(dmpe)_2]^+ + [MoH_4(dppe)_2]$$

This reaction occurs despite the fact that $[FeH(N_2)(dmpe)_2]^+$ and $[Mo(N_2)_2(dppe)_2]$ have $\nu(N_2)$ at 2094 and 1977 cm^{-1}, respectively, which by the criterion normally used implies that N_2 is more strongly bound to molybdenum than to iron.[9] The molybdenum-hydrogen binding presumably provides the driving force,

(1) Robson, R. L.; Eady, R. R.; Richardson, T. H.; Miller, R. W.; Hawkins, M.; Postgate, J. R. *Nature* **1986**, *322*, 388.
(2) Chisnell, J. R.; Premakumar, R.; Bishop, P. E. *J. Bacteriol.* **1988**, *170*, 27. Pau, R. N.; Mitchenall, L.; Robson, R. L. *J. Bacteriol.* **1989**, *171*, 124.
(3) See, for example: Postgate, J. R. *The Fundamentals of Nitrogen Fixation*; Cambridge University Press, 1982.
(4) See, for example: Müller, A., Newton, W. E., Eds. *Nitrogen Fixation*; Plenum Press: New York, 1983.
(5) Hills, A.; Hughes, D. L.; Jimenez-Tenorio, M.; Leigh, G. J. *J. Organomet. Chem.* **1990**, *391*, C41.
(6) Yamamoto, A.; Miura, Y.; Ito, T.; Chen, H.; Iri, K.; Ozawa, F.; Miki, K.; Sei, T.; Tanaka, N.; Kasai, N. *Organometallics* **1983**, *2*, 1429.
(7) Henderson, R. A.; Leigh, G. J.; Pickett, C. J. *Adv. Inorg. Chem. Radiochem.* **1983**, *27*, 197.
(8) An example of such a complex is $[\{Mo(C_6H_5Me)(PPh_3)_2\}\{Fe(C_5H_5)(Me_2PCH_2CH_2PMe_2)\}(\mu\text{-}N_2)]$: Green, M. L. H.; Silverthorn, W. E. *J. Chem. Soc., Dalton Trans.* **1973**, 301.
(9) For a discussion, see: Chatt, J.; Richards, R. L. In *The Chemistry and Biochemistry of Nitrogen Fixation*; Postgate, J. R., Ed.; Plenum Press: New York, 1971; pp 57-103.

0002-7863/91/1513-5862$02.50/0